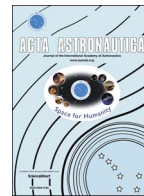




ELSEVIER

Contents lists available at ScienceDirect

Acta Astronautica

journal homepage: [www.elsevier.com/locate/actaastro](http://www.elsevier.com/locate/actaastro)

## Base pressure oscillations and safety of load launching into orbit

P.V. Bulat<sup>a</sup>, O.N. Zasukhin<sup>b</sup>, V.V. Upyrev<sup>b</sup>, M.V. Silnikov<sup>c,d,\*</sup>, M.V. Chernyshov<sup>c,d</sup>

<sup>a</sup> ITMO University, 49 Kronverksky Ave., 197101 St. Petersburg, Russia

<sup>b</sup> Baltic State Technical University, 190005 St. Petersburg, Russia

<sup>c</sup> Special Materials Corp., 194044 St. Petersburg, Russia

<sup>d</sup> Peter the Great St. Petersburg Polytechnic University, 195251 St. Petersburg, Russia

### ARTICLE INFO

#### Keywords:

Base pressure  
Self-oscillations  
Separated flow  
Rocket base  
Nozzle unit

### ABSTRACT

Physical details regarding base pressure low-frequency oscillations between rocket nozzles, their excitation and maintenance, are considered. Amplitude – frequency characteristics of these oscillations, as well as sequence of their type change, are studied. A single nozzle, a two-nozzle unit and a ring nozzle imitating multi-nozzle unit, are investigated in the present study.

### 1. Introduction

One of the key problems in spacecraft launching is the destruction risk of the carrier rocket due to unsteady interaction between supersonic jets emerging out of the multi-nozzle unit, and their affecting rocket base and the launch facility. This problem has been studied since 1950s, but some aspects are still unclear.

Physical details of base pressure low-frequency oscillations between rocket nozzles and their excitation and maintenance are considered in this study. Amplitude – frequency characteristics of these oscillations, as well as sequence of their type change, are studied. A single nozzle, a two-nozzle unit, and a ring nozzle imitating multi-nozzle unit, are studied. Nozzle units are installed inside a test channel having abrupt cross section expansion. The complex interaction between the exiting jet flows and the reverse flow produced upon their leaving the nozzles is studied.

It is demonstrated that the so-called expense mechanism underlies the oscillations. For some combinations of nozzle unit geometry and full pressure of the flow there is a misbalance between the two gas masses: one, which is ejected from a space near the rocket base, and a second, entering into this space from nozzle external flow. Results from experimental and computational investigation as reported here confirm this theory.

A model of the rocket base region, shown in Fig. 1, is composed of a high pressure reservoir (1) a nozzle (2) and a duct (channel) 3. The following geometrical parameters characterize the nozzle: the diameter of its critical cross-section ( $d_*$ ), its exit cross-section diameter ( $d_e$ ), the diameter of the duct (tube) section ( $d_t$ ), the nozzle throat angle ( $\theta_n$ ),

and the duct (tube) length ( $l_t$ ). Amplitude – frequency dependencies for base pressure ( $P_b$ ) oscillations are analyzed. Flow regimes, types of shock-wave structure oscillations and laws of their change due to full pressure ( $P_0$ ) variation are also studied here.

The very first experimental studies demonstrated that the unsteady effects associated with base pressure oscillations have significant influence on the vehicle supersonic flight. Meaningful changes in the load direction are a serious menace in supersonic vehicle constructions.

The loads are especially large at rocket engine jet interaction with launch facility surface, walls of launch container, jet – jet and jet – rocket base interaction. Typical steady and unsteady (oscillatory) flow regimes are shown in Fig. 2, above and below, correspondingly. Other facilities where shock-wave structure oscillations are typical also exist in spacecraft (ejector nozzles, for example). The problem of separated supersonic flow and associated base pressure oscillations is common for all of them.

#### 1.1. Background and history of studies of flows at the base region and base pressure oscillations

Among other problems of jet – obstacle interaction, problem of supersonic jet flow in channels with abrupt expansion has its separate place. Such flows, similar to reverse step flow, are realized in various engineering facilities (for example, in tubes of launch facilities, nozzles with abrupt steps, diffusers of the test benches for high altitude imitation, metallurgical furnaces, gas fittings and pipelines in chemical industry.

A large number of studies are dedicated to interior separated flows

\* Corresponding author at: Special Materials Corp., 194044 St. Petersburg, Russia.  
E-mail address: [mvcher@newmail.ru](mailto:mvcher@newmail.ru) (M.V. Silnikov).

<http://dx.doi.org/10.1016/j.actaastro.2016.11.042>

Received 21 November 2016; Accepted 27 November 2016

0094-5765/ © 2016 IAA. Published by Elsevier Ltd. All rights reserved.

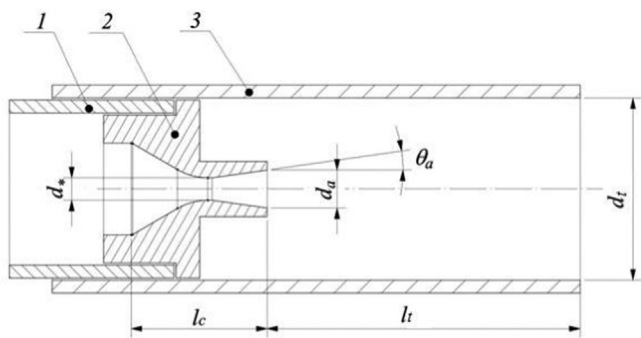


Fig. 1. The geometry of the duct with abrupt expansion: 1 – reservoir, 2 – supersonic nozzle, 3 – cylindrical tube. Here  $l_c$  is the nozzle length.

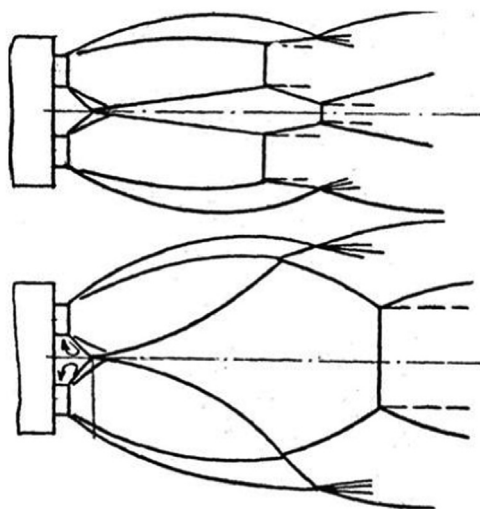


Fig. 2. Interaction of jet flows out of nozzle unit; for the steady regime (above) and oscillatory (below).

and associated base pressure variation. Nusselt was named as the first researcher of flows experiencing abrupt expansion [1]; he experimented with transonic jet flows out of the narrowing conical nozzles and compared his results with one-dimensional flow theory.

Numerous publications on jet flows at the base region, especially involving base pressure problems, appeared shortly after WWII [2–9]. Three steady regimes of ejector flow (mixed, transitional, and supersonic one) were discovered in conical and shaped nozzles with exit Mach number  $M_a=1.836$  [2]. A series of shadow (Schlieren) photos of the wave structures illustrated the flow regimes for the first time in that study. They demonstrated that as the reservoir pressure ahead of the nozzle increases, the base pressure initially decreases, and thereafter increases linearly after having some minimal value.

Attempts to achieve a reliable scheme of separating supersonic flow in the duct and to derive some numerical relations for the base pressure were undertaken in [10–12]. These studies contain research of sonic and supersonic jet flows in channels with abrupt expansion. Either shadowgraph photos showing the wave structure, or interferograms indicating various phases/regions of stream formation, are presented there. To define the range of self-oscillation existence and to exclude these self-oscillations was the goal of studies conducted at the beginning of the 1950s. But sometimes (for example, in metallurgy and for the hardening of materials) powerful low-frequency oscillations were useful and were applied to industrial practice.

More profound, detailed and comprehensive studies were provided later [13,14]. Base pressure – reservoir full pressure dependence  $P_b(P_o)$  was achieved for the axisymmetric duct of limited length [11]. Typical base pressure variations at the sonic nozzle flow were discovered, as well as hysteresis phenomena of shock-wave structure at

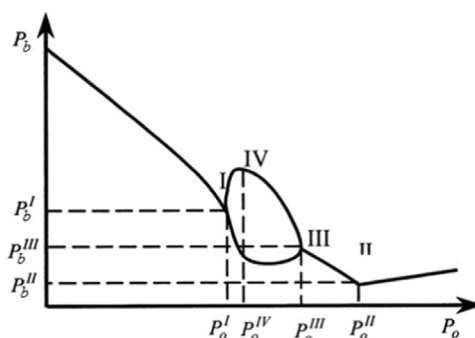


Fig. 3. Typical changes in the base pressure upon changes in the reservoir total pressure. Point I corresponds to the starting of self-oscillations, point II – to minimal base pressure, point III – to the end of oscillations, point IV – to maximum oscillations amplitude.

increase or decrease in the reservoir pressure. Low-frequency oscillations of the base pressure are discovered in [13]. As a result, the conception of  $p_b(p_o)$  dependence became basically modern (Fig. 3).

Outstanding studies of round and ring jet flows inside plane and axisymmetric ducts were provided in 1968–1980 [12–20]. Oscillatory base pressure regimes and shock-wave structure shift were discovered there experimentally using the fringe patterns in plane transparent channels and inertialess pressure sensors. W.M. Jungowski introduced the conception of “oscillations of the steady shocks” in his studies [12,13,21–24].

Non-classified publications on the topic appeared in the Soviet Union sometime later. But it does not mean absence of studies. Self-oscillatory interactions of supersonic jet flows faced with obstacles (parallel, normal to jet symmetry axis or inclined ones) were conducted in various organizations (TsAGI, Baltic State Technical University, Institute of Theoretical and Applied Mechanics of the Siberian Branch of the RAS, etc.). Some books (for example, [25,26]) and numerous papers were published.

O.N. Zasukhin [27] studied the flow pulsations in various nozzle sets. He confirmed W.M. Jungowski’s conclusion about the determining influence of shock-wave structure pulsations on the acoustic noise formation. Above it, so called flow rate mechanism of oscillations was stated, and it was proven that the acoustic feedback is subsidiary. This fact was substantiated by experimental studies of jet flow interaction with normal plane obstacles (Fig. 4).

Numerous theoretical, experimental and numerical studies performed in 1970s–1990s [28–32] had shown that the triple configuration of the shocks (at point T, Fig. 4) becomes unsteady and oscillates intensively between the nozzle and the obstacle. These oscillations occur at some specific jet flow parameters and distances between the

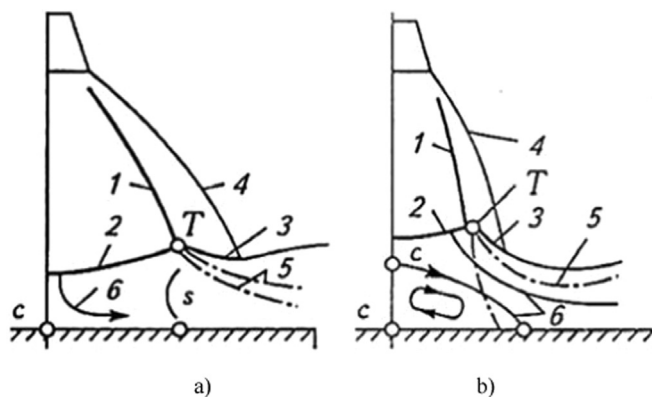


Fig. 4. Shock-wave structure of the supersonic jet at its interaction with a plane infinite obstacle: a) steady flow regime; b) flow with the central circulation zone; 1) “suspended” oblique shock; 2) central shock (Mach stem); 3) reflected shock; 4) jet boundary; 5) slipstream (mixing layer); 6) any streamline; s is sonic line; c is flow stagnation point.

obstacle and the nozzle exit section. A one-dimensional model of the oscillation cycle based on feedback, due to mutual interaction of shocks and other discontinuities (interior feedback) is proposed in [33]. At the same time, feedback via the ambient gas surrounding the jet flow (exterior feedback) is proposed and discussed in [34,35]. The perturbation caused by jet oscillations can propagate from the obstacle to the nozzle (via the ambient gas) and also in an opposite direction (via the mixing layer at the jet boundary). This type of feedback is confirmed when installing acoustical screens at the exterior side of the nozzle. Such screens eliminate this feedback and thereby change the oscillations' parameters.

Long-term discussion allows us to conclude a joint participation of both feedback mechanisms in self-oscillations. But the interior feedback seems to be prevailing, as it follows from the experimental study of supersonic jet self-oscillations at its flow about an obstacle in supersonic co-current stream [33]. This stream excludes the exterior feedback, but it does not prevent the interior one. So, it was proven that the basic mechanism of self-oscillations is the flow rate one (with the interior feedback).

## 2. Methodology of the experimental study

The system of dimensionless parameters determining the supersonic flow inside a duct with abrupt expansion can be written as it follows:

$$\Phi(P_0/P_a, P_b/P_a, F_t/F_a, l_t/d_t, \theta_a, M_a, W/d_t^3, T_a/T_0, A/P_0, f).$$

The values of  $P_0$  (stagnation pressure inside the reservoir),  $P_b$  (base pressure),  $A$  (base pressure amplitude), and  $f$  (the frequency of oscillations) are the set of the parameters measured experimentally.  $T_a$  (ambient temperature) and  $P_a$  (ambient pressure) are the surrounding measurable parameters. The set of the measured geometrical parameters of the experimental facility are  $d_a$  (nozzle exit section diameter),  $d_c$  (exterior diameter of the nozzle end),  $d_c$  (diameter of the critical nozzle section),  $\theta_a$  (nozzle throat half-angle),  $i$  (number of nozzles),  $d_n$  (distance between nozzles, for multi-nozzle units only),  $l_n$  (nozzle length);  $d_t$  (tube diameter),  $l_t$  (tube length),  $\alpha_t$  (throat half-angle of the expanding duct, for conical tubes). Other geometrical parameters of the experimental facility, such as  $F_c$  (area of the critical cross-section of the nozzle, or total one for all nozzles in a case of multi-nozzle unit),  $F_t$  (tube cross-section area),  $M_a$  (Mach number at nozzle exit section),  $W$  (volume of the base region) can be easily calculated. The total (stagnation) pressure inside the reservoir,  $P_0$ , is the only governing parameter.

Conical nozzles were manufactured for studying the jet flow inside the tube; it had a cross-section area of  $F_t=64.3 \text{ mm}^2$ . The nozzles had a fixed critical section area ( $d_c=10.6 \text{ mm}$ ) but different throat half-angles ( $\theta_a=8^\circ, 15^\circ, 30^\circ, 40^\circ$ ) and the flow Mach numbers varied from 1 to 5. Shaped nozzles ( $\theta_a=0^\circ$ ) resulted in a uniform stream at the nozzle exit section at the same Mach numbers. For more detailed studies experiments were conducted with lower Mach numbers, e.g., nozzles with  $M_a=1.1, 1.2, 1.3, 1.4, 1.5$  were also used.

In the experimental studies conducted with a single nozzle, the values of  $P_0/P_a, M_a, l_t/d_t, \theta_a$  were varied; the base pressure  $P_b$  was measured and an experimental plot like the one shown in Fig. 3 was plotted for the total and the base pressures. Similar studies were conducted with multi-nozzle units, but in these investigations two additional factors,  $d_n/d_c$  (see Fig. 5) and  $F_t/F_c$ , are to be added.

In the conducted experiments, flow visualization was done using plane transparent tube walls.

## 3. Methodology of calculations

Neither the amplitude, nor the frequency, or the oscillations' shape depends on turbulence parameters. This experimentally proven fact

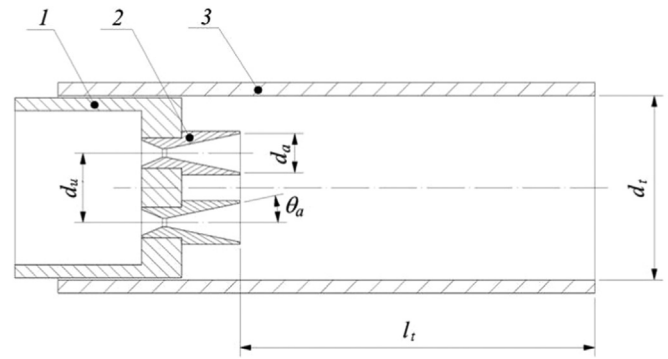


Fig. 5. Experimental facility (resonator) for multi-nozzle jet studies: 1 – reservoir and replaceable nozzle unit; 2 – replaceable supersonic nozzle; 3 – cylindrical tube (duct).

allows the adaptation of quasi-steady computational models. As shock-wave structure oscillations correspond to base pressure oscillations unambiguously, the base pressure is analyzed later.

Direct calculations of shock-wave structure oscillations using time-averaged Navier-Stokes equations supported with various turbulence models are difficult methodologically [36]. The Boussinesq hypothesis about turbulent viscosity underlies all two-parametric turbulence models allowing Reynolds averaging of Navier-Stokes equations. This hypothesis cannot be applied to complicated flows with large streamline curvatures or with boundary layer separation and reattachment, like in the considered case. Above all, time averaging is applied to the construction of turbulence models; therefore, their application to unsteady flow simulation is sometimes doubtful.

Nevertheless, flow simulation using turbulence models and time-averaged Navier-Stokes equations is acceptable, if the frequency of oscillations is much less than the characteristic frequency of vortex generation in turbulent flow. Base pressure oscillations can be considered as quasi-steady. This means that its period is much shorter than the typical time for gas-dynamical processes. It allows us, at least, to study oscillatory regimes qualitatively. But it is necessary either to solve the full Navier-Stokes equations, or to implement numerical method with explicit selection of shocks and other discontinuities.

Before starting the present calculations we tested the turbulence models that are widely represented in modern CFD tools, such as  $k-\omega$ , realizable  $k-\epsilon$ , RNG  $k-\epsilon$ , SAS, standard SST (Shear Stress Transport)  $k-\omega$  model and the transition SST model. Realizable  $k-\epsilon$  and the transition SST turbulence model proved to be the best for supersonic separated flows about the multi-nozzle units and rocket base parts. The first model provides reliable data on pressure distribution at the jet axis, the base pressure, pressure distribution at the nozzle and on the duct walls for small flow difference in the ambient space and at the nozzle exit section; even at rather coarse computational grid. The transition SST model provides better agreement with experimental results in cases where large pressures differences exist in the nozzle exit section and in the surroundings. It is more exacting to computational grid, boundary and initial conditions, requires sufficiently more time for calculations. At the same time, the transition SST model guarantees the qualitatively reliable results for shock-wave structure and acceptable accuracy of pressure distribution at the jet axis.

We performed calculations of the considered process as quasi-steady flow, and also as unsteady flow (the rate of total pressure variation was taken to be equal to 5 bars per second). As full pressure was increased linearly in our calculations, it is easy to transform  $P_b(P_0)$  calculated dependencies to  $P_b(t)$  pressure – time dependencies. But  $P_b(P_0)$  plots were first analyzed because they are easier to be compared with experimentally obtained results.

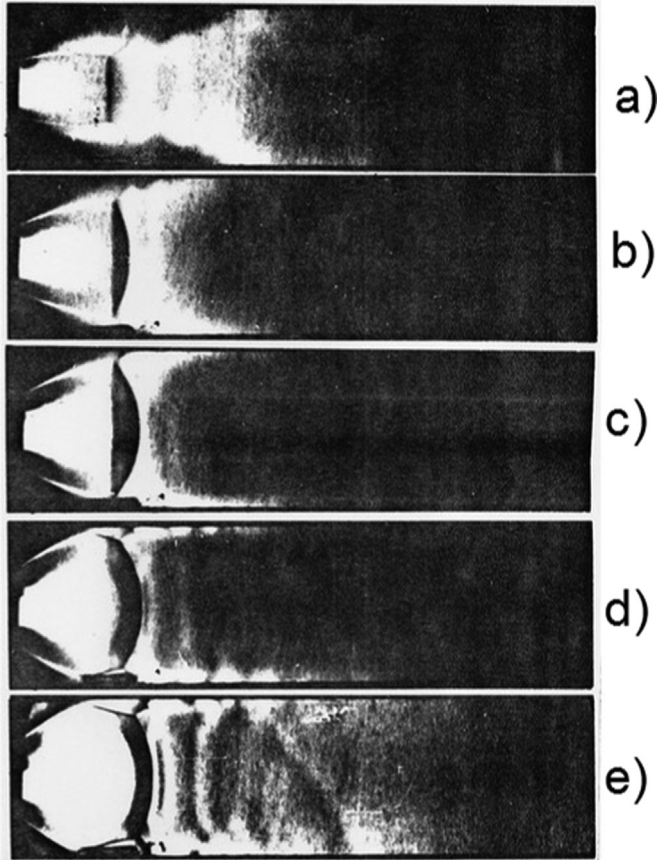


**Fig. 6.** Schlieren images of axisymmetric jet flow shock-wave structure transformation. Nozzle Mach number  $M_a=2$ ; channel walls are plane and transparent; the reservoir pressure increases from the upper to the lower images.

## 4. Results and discussion

### 4.1. Types of shock-wave structures in a duct with abrupt expansion for various flow regimes

In the present experiments, supersonic jet flow emerges out of ducts having either a planer or round nozzle. A plane nozzle imitated the two-nozzle unit to a certain degree. On the other hand, combination of plane nozzle and plane duct allowed avoiding distortion of the shock-wave structure experienced in the case where impingement of axisymmetric jet on plane walls takes place. Plane jet flow is unstable at low values of  $P_0$ ; it sticks alternately to different walls of the channel. Supersonic jets can result in different flow patterns; the flow remains axisymmetric and initially the jet sticks to the walls due to its turbulent nature (see Figs. 6a and 7a). As  $P_0$  increases, the diameter of this jet first “barrel” increases and reaches the diameter of the duct. The mixing layer of the jet begins to interact with duct walls and “bridge-like” shock appears. But the jet remains axisymmetric throughout the whole flow regime.

At the further increase of  $P_0$ , jet boundary shape remains unchanged, but the Mach stem decreases and moves farther away from the nozzle exit section (Fig. 6e). Double lines of the oblique shocks shown in Fig. 6 are a result of shock-wave interaction with the duct plane walls. Flow visualization allowed observation of the developed flow and wave patterns in a case of axisymmetric supersonic jet flow inside a cylindrical channel with abrupt expansion, for various flow regimes [37–39]. To specify the flow pattern, finite-volume CFD calculations were carried out. Transition SST turbulence model was used for completely unsteady flow simulation. As a result, five basic types of shock-wave structure were determined (Fig. 7) when compar-

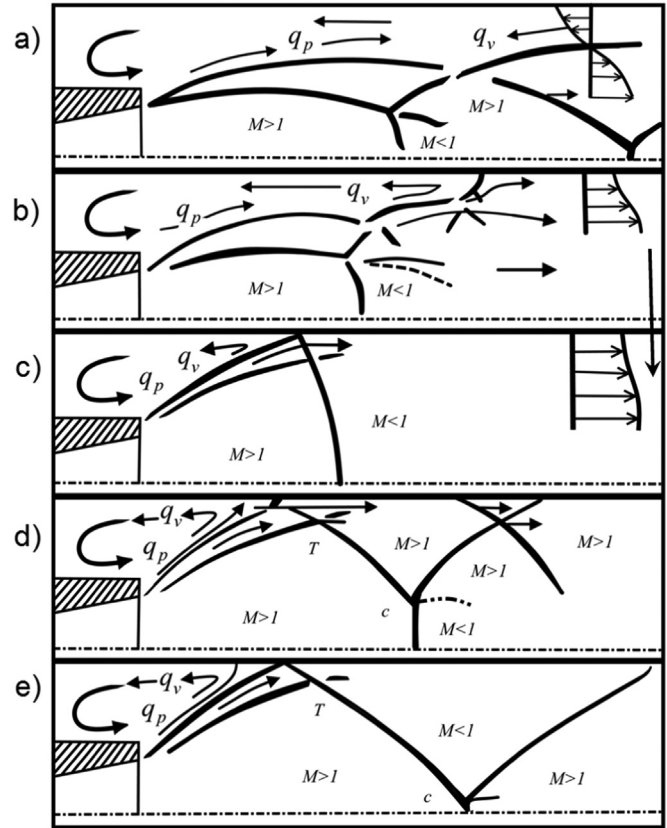


**Fig. 7.** Reconstruction of shock-wave structure resulting from axisymmetric jet flow emerging out of a round nozzle into a duct with abrupt expansion.  $q_p$  is a gas flow ejected from the base region,  $q_v$  is a gas flow penetrating into the base region,  $M$  is Mach number; the reservoir pressure increases from the upper to the lower images.

ing between experimental (Fig. 6) and numerical (Fig. 7) results.

All varieties of flow regimes can be divided into 2 large classes. There are flow regimes with an open base region (OBR, see Figs. 6a and 7a) and regimes with a closed base region (CBR, Figs. 6b–e and 7b–e). Examining Figs. 6 and 7, one can conclude that there are several CBR regimes. So?, the case when the jet interacts with the duct walls at its turbulent part, and the flow throughout the channel, from the impingement point is subsonic as shown in Fig. 7b. The case when bridge-like shock generates subsonic flow behind it is shown in Fig. 7c. This shock locks all duct cross section at jet impingement with duct wall. Later measurements of the base pressure and acoustic noise revealed that this flow regime corresponds to a minimum value of  $P_b$  and minimal level in the acoustic noise for a given nozzle Mach number and duct length. Further increase in  $P_0$  leads to formation of a reflected oblique shock (see Fig. 7d). This shock collides with another shock, at the first barrel of the supersonic jet (at point T, Fig. 7d), and reflects from the symmetry axis as a Mach stem. The flow downstream of the Mach stem is subsonic, but the flow along duct walls, including the oblique shocks, is completely supersonic.

Interaction of several supersonic jet flows out of a multi-nozzle unit leads to complex 3D structures. Additional elements of shock-wave structure were seen in shadowgraph visualization of the flow inside the duct while using plane transparent walls. Smearing the sidewalls of the cylindrical channel with mastic, we can determine the topology of the streamlines near sidewalls. These experiments were performed for cases in which the investigated nozzles were composed of two ( $N_n=2$ ) and four ( $N_n=4$ ) nozzle units. Photos of compound supersonic jet flowing out of 5 nozzles and 6 nozzles were taken. The 5-nozzle unit consisted of 4 nozzles situated at the corners of a square, and one nozzle situated at the center. For the latter case, nozzles were situated along circular line. We analyzed the shadowgraph photos and com-

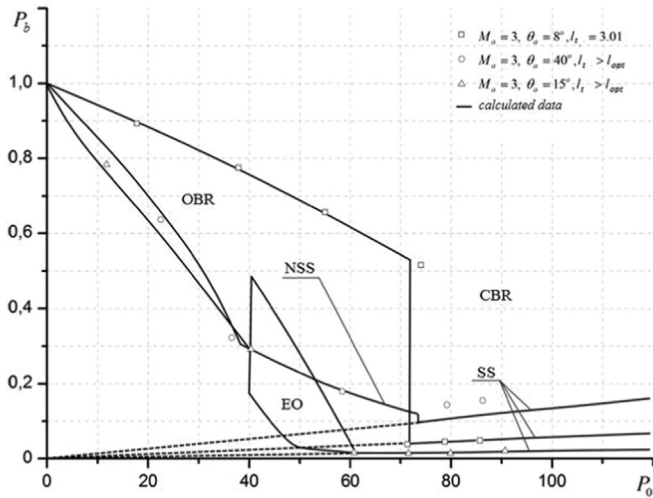


Fig. 8. Typical plot for  $P_b(P_0)$  dependence at various length of the duct;  $F_t/F_* = 64.4$ ,  $d_* = 10.6$ .

pared them with lines of mastic flow along the walls of a cylindrical channel. Flow with single ring nozzle can be compared with jet flow out of the multiple nozzles situated circularly. Interaction between neighboring jets is similar to the case in which the nozzles are situated in one row. Consequently, it is enough to study the structure of a single jet flow, flow out of two-nozzle unit, and ring jet flow to discover the basic physical flow features.

#### 4.2. Numerical and experimental determination of steady and unsteady flow regimes in flows emerging out of a single nozzle

Three typical experimentally obtained and calculated plots of  $P_b$  versus  $P_0$  for a single jet with Mach number  $M_\alpha = 3$  are shown in Fig. 8. It is evident that  $P_b(P_0)$  dependence can differ sufficiently from the plot in Fig. 3. Flow oscillations are not so pronounced at Mach number  $M_\alpha = 2$  at the nozzle exit (see Fig. 9). Self-oscillations do not appear at large nozzle angles, as well as at Mach number  $M_\alpha = 1$ . To investigate this feature, additional computations and experimental investigations of jet flows out of nozzles with  $M_\alpha = 3$ ,  $\theta_\alpha = 40^\circ$  and  $M_\alpha = 1$  were done. It was demonstrated that these jets have similar shape, large angle of first barrel expansion, and their corresponding plots for  $P_b(P_0)$  dependencies are very similar.

The experimental data presented here seem to be of interest;

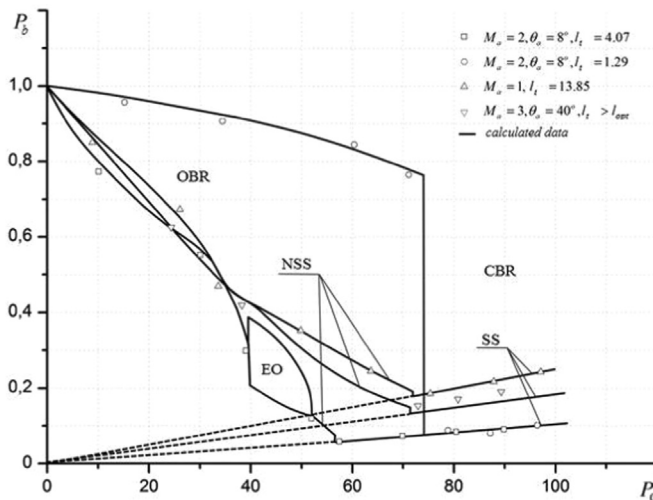


Fig. 9. Typical plot for  $P_b(P_0)$  dependence obtained experimentally;  $F_t/F_* = 64.4$ ,  $d_* = 10.6$ .

because they demonstrate three different  $P_b(P_0)$  types of correlation. An optimum tube length  $l_t = l_{opt}$  exists; it corresponds to absolute minimum of the base pressure at any given duct diameter. If  $l_t < l_{opt}$ , the duct is too short, and the plot for  $P_b(P_0)$  qualitatively corresponds to the upper curve in Fig. 8. If  $l_t > l_{opt}$ , then the duct is medium or too long, and the plot corresponds to the lower curve in Fig. 8. The shorter is the tube, the lower is the descending line of the plot. Characteristic values of  $P_b$  and  $P_0$  decrease, as the duct becomes shorter. This continues until  $l_t = l_{opt}$ ; thereafter, characteristic values of these pressures increase. According to the experimental data, the optimum length of the duct is approximately equal to the following value:

$$l_{opt} = \frac{3, 15}{2(0, 7 + \tan \theta_\alpha)} M_2 d_t.$$

It is convenient to apply  $P_b(P_0)$  plots to flow regime classification. All regimes are present at flow in long ducts. It is worthy of note that the base pressure depends linearly on the full pressure at self-similar mode; the straight line comes from the start of coordinates, and it corresponds to the constant jet incalculability. This is the reason why this flow regime was named self-similar (SS). All other regimes are not self-similar (NSS), i.e. the channel flow depends on ambient conditions. The region of the “flow rate” oscillations (EO) is situated between OBR and NSS modes at moderate nozzle angles. Some transition processes accompanying the change of basic regimes, also can be seen. All regimes can be classified as steady and unsteady. The unsteady regimes, in turn, can be divided into transitional and oscillatory.

Detailed analysis of the experimental data has shown that there are five types of oscillations: two types of high-frequency stochastic oscillations (at the transitions from OBR to NSS and from NSS to the region of flow rate oscillations), and three types of low-frequency oscillations of “flow rate” origin (CO – composite oscillations, PHO – pseudo-harmonic oscillations, RO – relaxation oscillations).

#### 4.3. Experimental study of steady and unsteady regimes in the flow emerging out of a two-nozzle unit

The jet that flows out of a two-nozzle unit into a duct with sudden expansion is a good model of a compound jet; it is an elementary cell of more complex compositions. The interaction of two jets that flow out of a two-nozzle unit is the same as between two adjacent jets in a multi-nozzle unit. On the other hand, many flying vehicles have just two nozzles. Layout of the experimental facility where studies were conducted is shown in Fig. 5.

Distribution of flow parameters at the volume of the base region cannot be considered as uniform even approximately. Interactions of mixing layers and supersonic streams with walls differ significantly at the plane of axis of the nozzles and at the plane that is normal to them. All base area can be divided into two communicating volumes: first, the zone between nozzles, and second, the remaining part. Flow visualization demonstrates that volume and shape of the zone between nozzles is almost invariable both in steady, and in unsteady flow regimes, neglecting total pressure variations. It is the peripheral flow region that “breathes”.

As stated above, self-oscillations do not appear in flow out a single axisymmetric nozzle at  $M_\alpha = 1$ . But the experiments with the two-nozzle unit revealed development of oscillations similar to the case of a single jet at  $M_\alpha = 2$  (Fig. 10). The reason for self-oscillations excitation is as explained in the following. Two closely situated jets transform into an almost round turbulent jet that is similar to the round jet flow out of the nozzle with  $M_\alpha = 2$  and  $\theta_\alpha = 8^\circ$ . The similar variation of  $P_b(P_0)$  has the same reason. If the nozzles are situated with a long distance between them, jets interact weakly, and the  $P_b(P_0)$  plot is reminiscent of the case of single jet flow out of a single nozzle with  $M_\alpha = 1$ .

The most developed oscillatory single nozzle flow regime forms at  $M_\alpha = 3$ , and  $\theta_\alpha = 15^\circ$ . The subsequent experiments were conducted with such nozzles. As nozzles are situated close one to another, jet rather

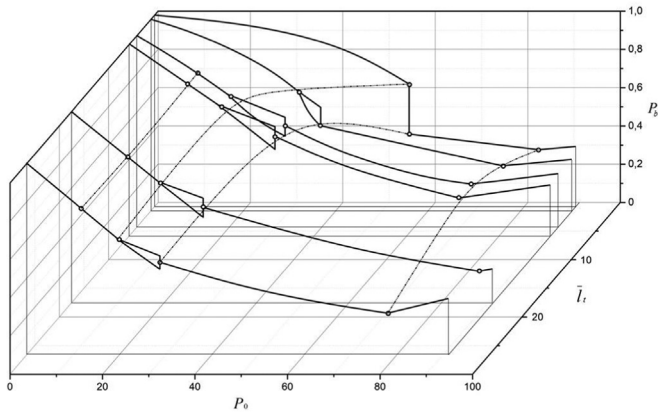


Fig. 10.  $P_0(P_b)$  dependence at  $d_n=0.471$ ,  $M_a=1$ .

quickly transforms into round one and leads correspondingly. If nozzles are situated at large distances from each other, then self-oscillations appear as in a single nozzle, but the amplitude dependence on  $P_0$  is qualitatively different. For the case of single nozzles, oscillations start immediately with large amplitude; this amplitude decreases gradually as  $P_0$  increases. In the case of two-nozzle units, amplitude is close to zero at the start of self-oscillations; at first, it grows as  $P_0$  increases and, after a maximum, it decreases.

The conducted experiments lead to the realization that there are two oscillatory mechanisms which correspond to jet flow – wall interaction in two orthonormal planes, when two parallel jets flow into the duct with sudden expansion. This hypothesis was completely confirmed in experiments conducted with  $d_n=0.708$  (Fig. 11).

Fig. 11 demonstrates that there are two separate oscillatory regimes, corresponding to shock-wave structure oscillations in two orthonormal planes. It is apparent that the greater is the distance between nozzles, the stronger is the shift. This effect is not visible in the short tube cases.

It is interesting that aspects of two-nozzle jet flow with  $M_a=2$  are intermediate between the above-mentioned situations ( $M_a=1$  and  $M_a=3$ ). Oscillatory regime appears everywhere, superposition of two oscillatory modes is very pronounced, the plot of  $P_b(P_0)$  dependence is deformed seriously at the oscillatory regime, but there is now a split of the oscillatory regime into two separate regimes.

Thus the performed study of shock-wave processes that accompany two parallel jet flows into the channel with abrupt expansion allows us to make some important conclusions.

General principles for this flow are the same as in the case of a single nozzle. The dependence of  $P_b(P_0)$  is similar to what was observed in the case of single nozzle flow. The shape of the jet differs sufficiently from the case of a round jet flow out of a single nozzle.

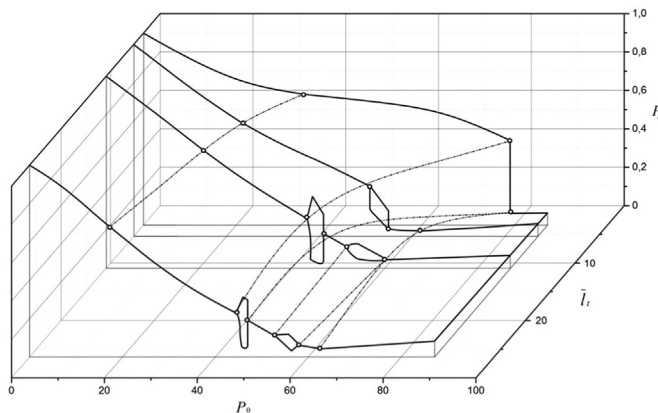


Fig. 11.  $P_0(P_b)$  dependence at  $d_n=0.708$ ,  $M_a=3$ ,  $\theta_a=15^\circ$ .

Consequently, the conclusion is that self-oscillations do not appear in a jet flows when  $M_a=1$ , and when  $M_a=3-4$  and  $\theta_a=40^\circ$  do not apply in the case of two-nozzle units. In addition, the oscillatory regime looks more complex. It consists of two separate oscillatory modes. Those modes can be superimposed, or exist separately, depending on the range of total pressure  $P_0$ .

#### 4.4. Numerical analysis of the oscillatory cycle

##### 4.4.1. Jet flow out of the ring nozzle

Ring jet flows into the channel with abrupt expansion are of interest as a model of the compound jet flow out of the nozzles situated circularly. It is evident, that features of the ring jet are reminiscent of the features of ordinary jet flow out of a Laval nozzle with round cross-section. But differences are also possible, because of the interior base region presence, and it is always closed, but the peripheral base region can be open as well as closed. We can compare the typical plots for  $P_b(P_0)$  dependence in a ring jet and in an ordinary jet. It is necessary to make clear, whether any new flow regimes appear in ring jet flows. Do the oscillations of base flow in interior or peripheral base region exist? Do the self-oscillations look alike as in the case of an ordinary single axisymmetric jet?

Layouts for computational studies are presented in Fig. 1 (ordinary single jet), and in Fig. 12 (ring jet flow). Experimental data for ring jet flow into the duct with abrupt expansion are absent, so the comparison with the case of the unit of six nozzles was carried out. The following geometrical parameters were used for ring flow calculations: nozzle Mach number  $M_a=2$ ; critical diameter of the Laval nozzle  $d_{*1}=15$  mm, critical diameter of the ring nozzle  $d_*=5.3$  mm, diameter of the middle line of the ring jet  $D_*=21.25$  mm, exterior diameter of ring nozzle exit  $D_a=25$  mm, nozzle angle  $\theta_a=8^\circ$ , relative length of the duct  $l_t=L_t/d_t=4.02$ , its diameter is the same as in the case of single jet ( $d_t=85$  mm). Non-sticking and non-penetrations conditions are applied for the symmetry axis, condition of sticking and non-penetration – at solid walls. Number of cells in the nozzle critical section is not less than 40. The solution was conducted as axisymmetric on a structured grid with quadrangular cells. The considered flow field is completely unsteady. The calculations are completely unsteady, because they are done for oscillatory flow studies. The unsteady state calculations bring to life the problem of accumulation of numerical errors. If the code is properly assembled it does not allow systematic or periodic errors – only stochastic errors are possible. Special investigations showed that stochastic errors accumulate proportionally to the square root of the number of time steps. Thus for each accuracy of calculations there exists the maximal allowable number of time steps for the accumulated error should not exceed the allowable value [40,41]. The current

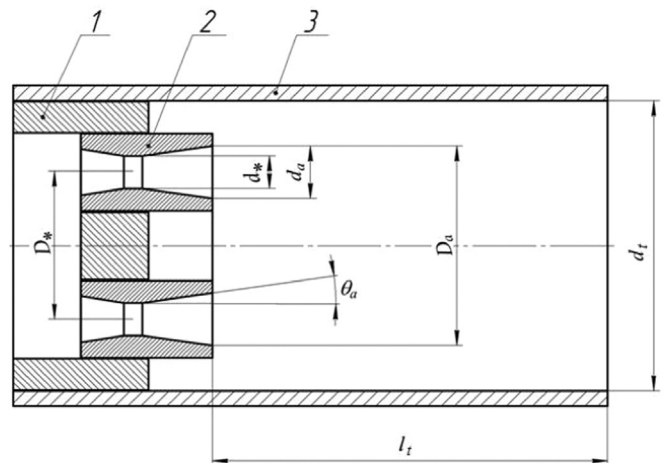
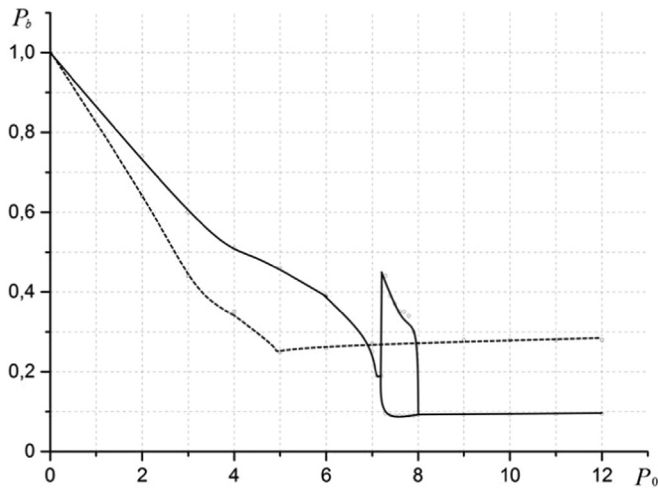


Fig. 12. Layout of the jet flow out of a ring nozzle into the channel with abrupt expansion: 1) nozzle unit; 2) ring nozzle; 3) channel (tube, or duct).



**Fig. 13.**  $P_b(P_0)$  dependencies on the central base region and the peripheral one (solid and dashed lines, correspondingly).

simulations did not allow accumulation of error exceeding 5% based on estimates following methodize developed in [40,41].

Unlike the case of flow from a simple Laval nozzle, now we see two base regions near the ring jet: the central one and the peripheral one. Correspondingly, different dependencies for  $P_b(P_0)$  characterize these regions (see Fig. 13). It is clear from Fig. 13 that there is a marked difference between the  $P_b(P_0)$  curves obtained for the interior (central) base regions and for the peripheral regions.

Oscillations in the interior base region are not excited. The interior (central) base region becomes closed very soon after nozzle start. The mixing layer at the interior side of the ring jet touches the symmetry line at  $P_0=3$  bar, so the bend in the  $P_b(P_0)$  plot can be seen at the dashed line in Fig. 13. Parts of the ring jet begin to interact at  $P_0=5$  bar. The minimal pressure in the central base region corresponds to this flow feature. The base pressure in the central zone increases slowly and linearly with increase in the reservoir pressure. The reason for this is the division of the interior base region from the ambient surroundings by the supersonic flow zones, and the interior base pressure does not depend on the exterior one.

It is also interesting to compare  $P_b(P_0)$  dependencies at the peripheral base region of the ring jet and at the base region of the ordinary (round) jet. The base region in the axisymmetric jet is larger than that of the ring jet peripheral base region. So the shift to NSS mode with the closed base region occurs at higher values of  $P_0$ , the duration of self-oscillatory cycle is smaller, and base pressure at self-similar mode is higher. It is worthy to mention also that the ring jet has a long, though weakly pronounced, sector between low-frequency oscillations and self-similar mode.  $P_b(P_0)$  dependence remains non-linear at that sector of the ring flow, but it becomes linear just after the point of minimal base pressure for the simple round jet. This phenomenon can be explained by the separation of the exterior jet boundary flow from the duct walls (Fig. 14). At the separation, disturbances from the ambient media penetrate into the peripheral base region. At regimes with closed base region, flow sketches look alike one another, but the central shock curvature direction is to the nozzle in the ring jet flow, and it is curved from the nozzle at the

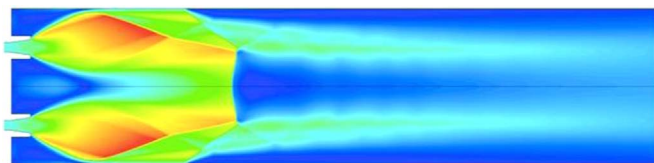


**Fig. 14.** Sketches of jet flows out of the ring nozzle (Mach number  $M_a=2$ ) into the duct with sudden expansion.  $P_0=10$  bar.

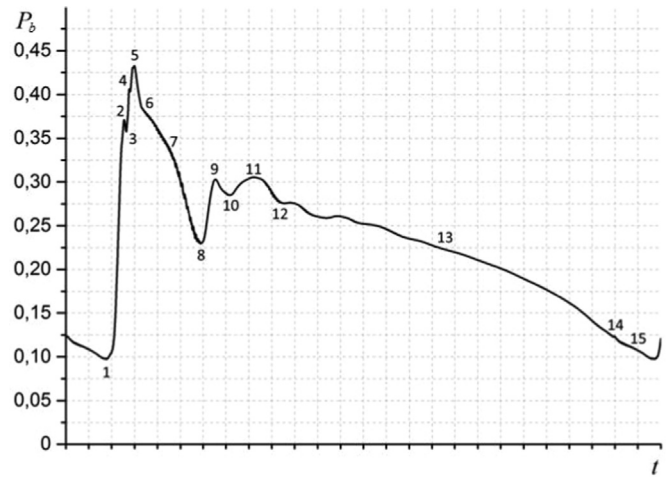


**Fig. 15.** Layout of a flow oscillatory cycle. Marked key points correspond to flow sketches shown in Fig. 16.

ordinary round one.

Let us consider the features of the oscillatory cycle in ring jet flow. Completely unsteady and quasi-steady CFD computations confirmed the quasi-stationary type of low-frequency oscillations once again. Variation in the base pressure, during one oscillatory cycle at the start of the oscillatory regime, is shown in Fig. 15. Marked points appearing in Fig. 15 along the composite oscillatory flow cycle correspond to the flow illustrations shown in Fig. 16.

Let us be reminded that the oscillations are designated as composite, because part of the cycle occurs at CBR, and another part occurs at OBR. Oscillations at the central base region are absent. It can be seen, that the oscillations in the peripheral base region completely corresponds to typical composite oscillations, starting at single round jet flow to the channel with abrupt expansion. But interior shock-wave structure differs significantly; this is due to the presence of a central base region and jet boundary. Above all, the interior base pressure volume remains approximately constant, but the peripheral base region “breathes”. As the exterior jet boundary strikes the channel walls, composite conical shocks are being generated. They reflect from the symmetry axis as a concave Mach stem.

As  $P_0$  increases, the shape of the oscillatory cycles are preserved but their frequency becomes higher. At a total pressure of 7.6 bar, the oscillatory cycle becomes shorter, and its frequency redoubles. Part of the cycle between points 8–13 (Fig. 15) disappears, and a new cycle completely similar to composite oscillations begins at once. So, two oscillatory modes superimpose. The first corresponds to composite oscillations, the second, to pseudo-harmonic oscillations. As  $P_0$  increases further, composite oscillations transforms to pseudo-harmonic, and all oscillatory cycles occur at the closed base region. The frequency of the pseudo-harmonic oscillations is approximately twice that of the composite oscillations frequency. Amplitude modulation appears at higher values of  $P_0$ . Different base pressure slashes? interchange every second period of oscillations. But the pressure splash amplitude at the first oscillatory cycle remains constant; the amplitude of the splash in the second cycle decreases and disappears (relaxation of oscillations).

So ring jet flow into the duct with abrupt expansion is, on the whole, similar to ordinary (round) jet flow. But the presence of an interior base region transforms the typical plot of  $P_b(P_0)$  and the shape of the oscillatory cycle.

#### 4.4.2. Ordinary (round) axisymmetric jet

Flow oscillation analysis is performed for the simpler case of a single round jet. Concept of misbalance of mass flow rate  $\xi=(q_p-q_v)/Q_a$  is introduced. Here  $Q_a$  is gas mass flow rate through the nozzle,  $q_v$  is the mass flow rate of gas penetrating into the base region from the

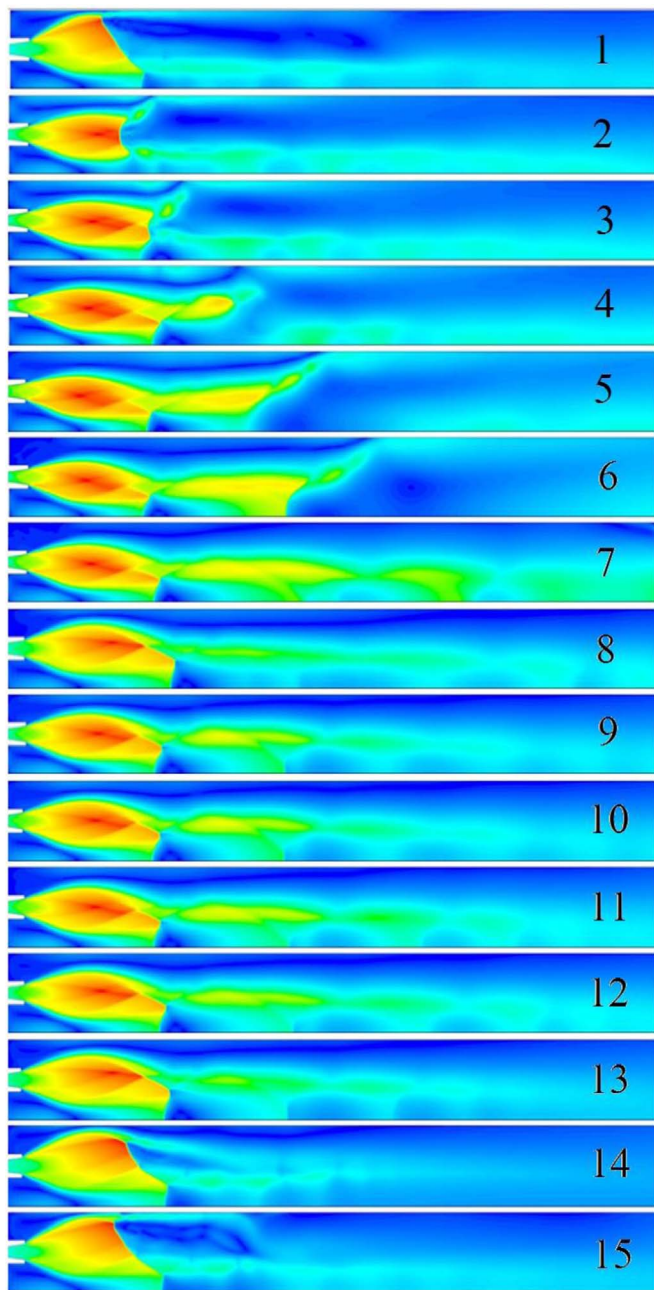


Fig. 16. Flow diagrams (the upper halves of ring jet flow) during a single period of flow oscillations.

ambient media or from the region where jet boundary sticks the sidewall,  $q_p$  is the mass flow rate that the jet ejects from the base region (see, for example, Fig. 7).  $\xi$  is the criterion that characterizes the performance of the considered mechanical system.

Calculating the mixing layer – sidewall interaction or the parameters of the inverse flow at OBR regimes, one can estimate also  $q_w$  and  $q_p$ , and determine also the misbalance  $\xi$ . If the misbalance is equal to zero for a given  $P_0$ , the system is steady; otherwise, the base pressure changes. If the function  $\xi(P_b)$  has no roots within the range of realizing values of  $P_b$ , the system (jet in a duct) cannot be steady at a given  $P_0$ . Variations in the total pressure result in rearrangement of the shock-wave structure, a birth and destruction of limit cycles, and various transitional processes. Calculated results for  $\xi(P_b)$  and corresponding phase trajectories of the oscillatory cycle are given in Fig. 17. The case of absence of oscillations is shown in Fig. 18.

Variations in the base pressure during the oscillation period

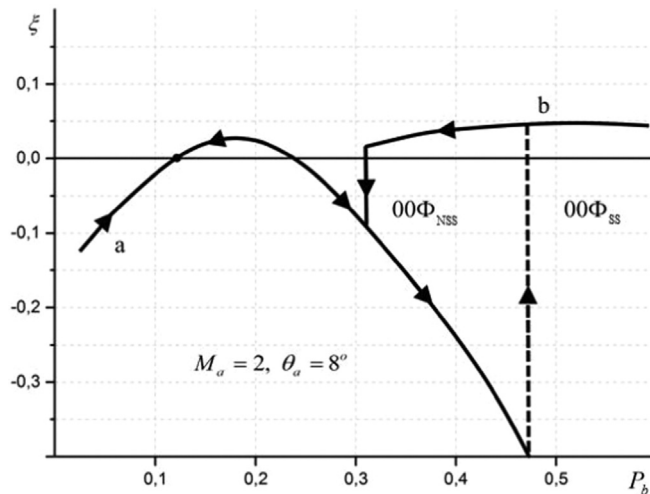


Fig. 17.  $\xi(P_b)$  dependence calculated at the oscillatory flow regime.

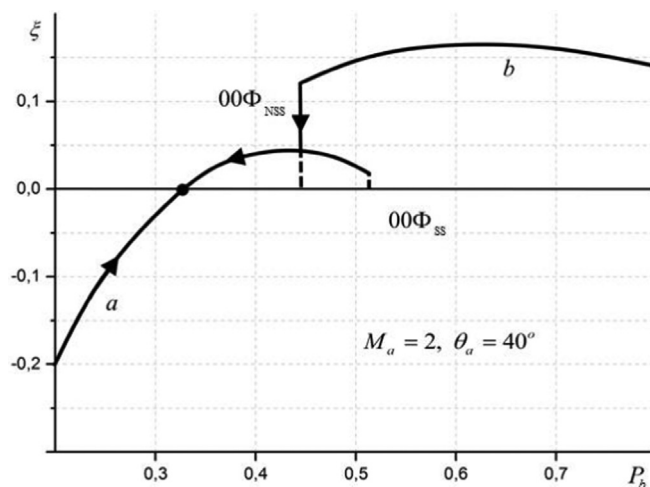


Fig. 18.  $\xi(P_b)$  dependence calculated at non-oscillatory flow regime.

corresponds to movement of calculated points along closed phase trajectories in a region where the dependence  $\xi(P_b)$  is ambiguous. For steady (non-oscillatory) regimes phase trajectory leads to stable situation  $\xi(P_b)=0$  marked by points in Figs. 17 and 18. Corresponding calculated and experimental data are shown in Fig. 19.

In experimental studies of oscillatory regimes, the total pressure  $P_0$

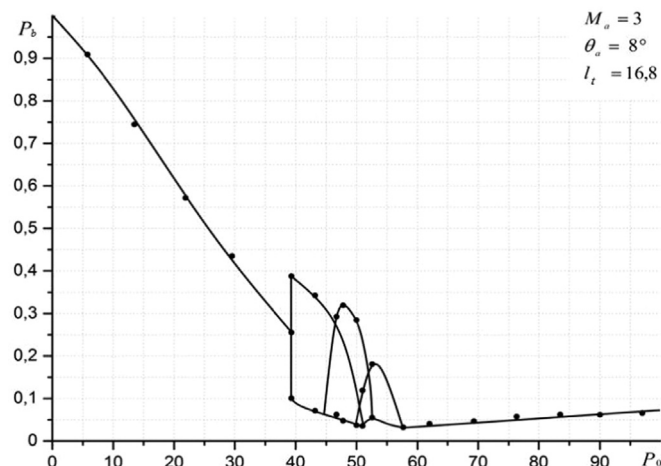
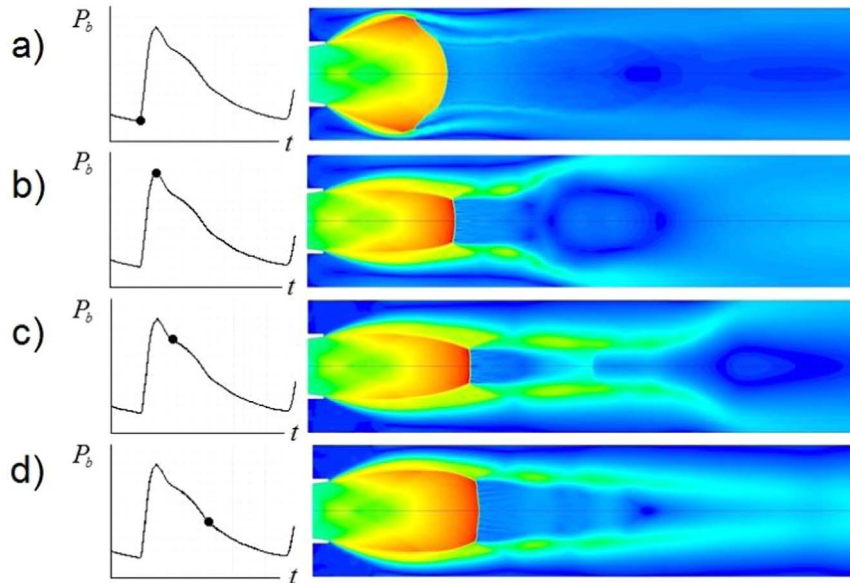


Fig. 19.  $P_b(P_0)$  dependence obtained numerically (solid lines) and experimentally (points).



**Fig. 20.** The oscillatory regime and shock-wave structures corresponding to composite oscillations at  $P_0=42$  bar.

was changed slowly enough to visualize shifts from any type of oscillation to another one. It was shown that different types of oscillations are superposed, i.e. the transitional region corresponding to different types of oscillations exists. As  $P_0$  increases, composite, pseudo-harmonic and relaxation oscillations replace one another successively. Let us consider the shape of the oscillatory cycle and other features of those types of oscillations.

A sequence of photos characterizing the oscillatory cycle at the regime of composite oscillations is presented in Fig. 20. At the left-hand side, one can see  $P_b(t)$  plots; the flow structure at these points is shown on the right-hand side.

#### 4.4.3. Analysis of the oscillatory processes

Creation of a misbalance between the two gas masses (ejected from the base region and penetrating from the ambient zone) at some total pressure value seems to be the reason for excitation of the oscillatory mode. Misbalance exists at any value of the base pressure; this feature supports the oscillatory mode. Such mechanism of oscillations is named an “flow rate” one. Analysis of a composite oscillatory cycle using the concept of gas flow rate misbalance is presented in Fig. 21.

The unambiguity zone is seen at the phase plane  $\xi(P_b)$  in Fig. 21;

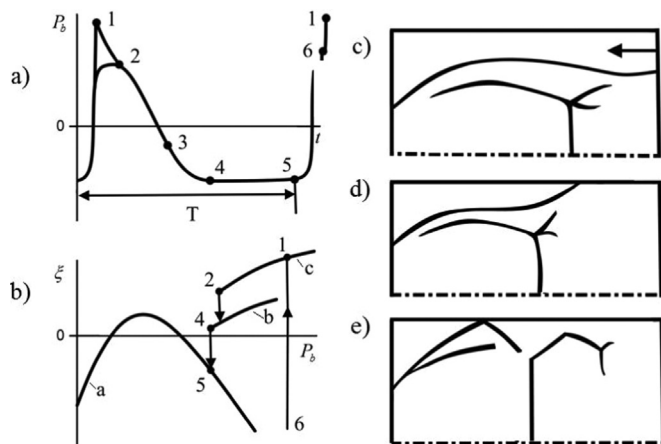


**Fig. 21.** Analysis of oscillatory cycle at composite oscillatory regime: curve a –  $\xi$ - $P_b$  dependence at initial jet part interaction with duct wall; curve b –  $\xi$ - $P_b$  dependence at OBR flow mode; curve c –  $\xi$ - $P_b$  dependence on the turbulent part of the jet interacting with a sidewall.

three different values of  $\xi$  correspond to the same value of  $P_b$  in this zone. It is a region of self-oscillations. The characteristic points 1–6 are marked at  $P_b(t)$  in Fig. 21a. Corresponding points are presented at  $\xi(P_b)$  diagram (Fig. 21b), as well as the layouts of shock-wave structures (Fig. 21c-e). The upper curve  $\xi(P_b)$  (Fig. 21b, points 1 and 2) corresponds to turbulent jet flow about the sidewall (it is shown in the middle layout of the shock-wave structure, Fig. 21d). The middle curve corresponds to OBR flow (corresponding shock structure is shown in Fig. 21c). Both cases correspond to gas exhausted from base region ( $\xi > 0$ ). The lower curve corresponds to the situation when initial part of the jet impinges a wall (Fig. 21e).

The oscillatory cycle looks as follows. Let the jet be initially situated at point 5 (Fig. 21). Shock-wave structure with OBR corresponds to this point (see Figs. 21c or 20d). The jet intensively ejects gas from the base region; its size increases quickly until it touches a wall at its initial part (Fig. 20a and point 5 in Fig. 21). Jet rearrangement to situation 5–6 (initial part of the jet flows about a wall, Fig. 21e) occurs later. Flow rate misbalance is positive and very large there. As the flow impulsively penetrates into the base region, the initial part of the jet detaches from wall, and the point of jet boundary – sidewall interaction shifts into the turbulent part of the jet (Figs. 20b, c, 21d). The upper (1–2) curve  $\xi(P_b)$  in Fig. 21b corresponds to this process. Thereafter, the turbulent part of the jet also leaves the wall and ambient gas penetrates into the base region (Figs. 20e, 21c, middle curve  $\xi(P_b)$  and arrow 4–5 in Fig. 21b). Afterwards, the cycle repeats.

Pseudo-harmonic oscillations differ from the composite – OBR part of oscillatory cycle is absent. Oscillations occur at closed base region. Flow oscillates between two extreme situations. The first of them corresponds to the turbulent part of the jet striking on a sidewall, the second one – to the interaction at the first barrel of jet flow with duct walls. The observed shape of the pseudo-harmonic oscillatory cycle is similar to that of the van der Pol oscillator (Fig. 22).

Since the jet interacts with the duct wall at its turbulent part, the base region empties and points of jet boundary strike the sidewall close to the nozzle. As the jet touches the wall at its first barrel, the base region fills impulsively and a jet boundary comes off a wall. Thereafter, the cycle repeats.

As  $P_0$  increases in the pseudo-harmonic oscillatory mode, modulation of amplitude starts. The reason for the modulation is as following: The maximal cross-section of the initial part of the jet comes too close to the duct wall, and a long vertical flow region appears between that section and the section where the turbulent part sticks to the wall.

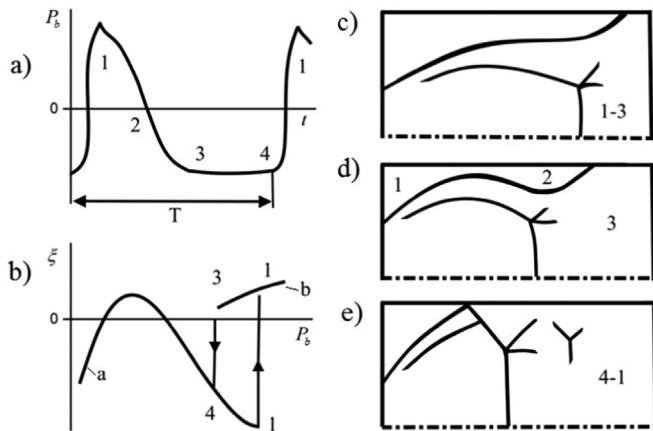


**Fig. 22.** Analysis of oscillatory cycle at pseudo-harmonic oscillations: curve a –  $\xi$ - $P_b$  dependence at initial jet part interaction with duct wall; curve b –  $\xi$ - $P_b$  dependence at turbulent part interaction with a sidewall.

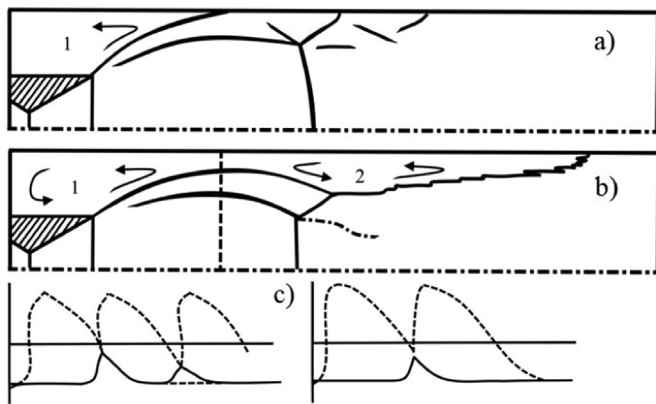


**Fig. 23.** Analysis of oscillatory cycle at pseudo-harmonic mode: 1) base region; 2) stagnation region.

Upon further increase in  $P_0$ , this region start “breathing” with a frequency approximately equal to the frequency of pseudo-harmonic oscillations; so, the second mode of oscillations appears. Those two pseudo-harmonic oscillatory cycles with some phase shift superimpose, and the total frequency doubles. Base pressure gradually stops being dependent on the ambient conditions because the base region basically exchanges gas masses with the stagnation region 2 (Fig. 23). So, one of two modes gradually reduces its amplitude at  $P_b(t)$ . Since that amplitude becomes equal to zero, pseudo-harmonic oscillations end, and the relaxation oscillations start.

Generation and disappearance of the second stagnation vertical flow region (zone 2 in Figs. 22d and 23b) accompany the relaxation oscillations. A vortex in region 2 is “locked” due to supercritical flow relation in zone 2 and the base region 1. It destructs the upper part of the cycle (dashed line in Fig. 23) and shifts the process to the descending branch; it is similar to ejection from a surrounding media at a supercritical flow regime. As a result, the oscillatory cycle looks like a saw (Fig. 23c). The horizontal “shelf” of the plot corresponds to gas exhaust from a base region 1 (Fig. 23b). The ascending branch corresponds to the filling of the base region, as the jet initial part flows about a sidewall (Fig. 23a). As  $P_0$  increases, the upper point of the oscillatory cycle, which corresponds to “choking” of the vertical flow 2, shifts along the descending branch of the plot. Correspondingly, the frequency of self-oscillations decreases.

#### 4.4.4. Termination of self-oscillations

As a rule, low-frequency oscillations diminish near the point corresponding to the minimal base pressure. Let us fix the value of

$P_0$  at this moment and consider whether the amplitude of oscillations would decrease to zero, or it would remain constant? A series of experiments conducted with variations in  $P_0$  revealed that such a transitional process really exists. Its duration is, as a rule, about 5 time periods of the low-frequency oscillations. Three pairs of  $P_b$  splashes with amplitude smaller than the amplitude of non-disturbed oscillations are usually present during this time interval. The time between pressure peaks is approximately equal to  $2T$  ( $T$  is the period of oscillations). Thereafter, the oscillation amplitude decreases during the time  $T$  to the amplitude of chaotic pulsations of the base pressure. Amplitude of any following pulsations is smaller than the amplitude of the successive preceding one by approximately 2.5 times.

## 5. Conclusion

Supersonic separated flows with base region presence and intense low-frequency oscillations appearing at such flows are considered in the present study. Intense self-oscillations at rocket base regions can lead to their destruction and to subsequent accidents.

Flows out of one nozzle, two nozzles and nozzle sets placed along a circle, including the ring nozzle, are considered. Jet flows out of these nozzle units to the channel with abrupt expansion are studied experimentally and numerically. It is shown that there are three types of low-frequency oscillations. The mechanisms supporting such oscillation types differ, but the feedback is the same (interior, or “flow rate” one). The acoustic feedback does not influence the excitation of oscillations, therefore one should control the gas masses penetrating into the base region.

At ring jet flow, pressure oscillations in a base region between exterior nozzle contour and duct wall (or exterior supersonic flow in real flow conditions) are, on the whole, similar to oscillations exciting around a single de Laval nozzle. Oscillations do not appear in the interior base region (between base of the nozzle unit, interior nozzle contour and the interior jet boundary).

As two-nozzle flow was studied, it was disclosed that the oscillatory mode is, in fact, a superposition of oscillations in two planes normal to one another. If the nozzles are situated far from each other, two separate oscillatory regimes, existing in different ranges of the reservoir pressure, can appear.

Self-oscillations do not depend on jet flows with Mach number close to unity emerging out of nozzles with throat angles  $\theta_a > 40^\circ$ . Shape of the function of flow rate misbalance in the base region, that depends on the total (reservoir) pressure, can predict, whether the self-oscillations are to appear.

The study allowed us to determine the reasons and structure of rocket base flow oscillations, as well as to acquire a tool for their control, including the full prevention of oscillatory flow regimes.

## Acknowledgement

This work was financially supported by the Ministry of Education and Science of the Russian Federation (agreement No 14.578.21.0111, a unique identifier of applied scientific research RFMEFI57514X0057).

## References

- [1] L. Crocco, *One-Dimensional Treatment of Steady Gas Dynamics*, in: H.W. Emmons (Ed.) *Fundamentals of Gas Dynamics*. Vol. III: High Speed Aerodynamics and Jet Propulsion, Princeton University Press, Princeton, New Jersey, 1958, pp. 110–130.
- [2] E.P. Neumann, F. Lustwerk, High-Efficiency Supersonic Diffusers, *J. Aeronaut. Sci.* 18 (6) (1951) 369–374.
- [3] E.P. Neumann, F. Lustwerk, Supersonic diffusers for wind Tunnels, *Trans. ASME J. Appl. Mech.* 16 (2) (1949) 195–202.
- [4] D.R. Chapman, An analysis of base pressure at supersonic velocities and comparison with experiment, *NACA TN 2137* (1950) 70.
- [5] J. Lukaszewicz, Diffusers for Supersonic Wind Tunnels, *J. Aeronaut. Sci.* 20 (9) (1953) 617–626.
- [6] J. Fabri, R. Siestrunk, Supersonic air ejectors, *Adv. Appl. Mech.* 5 (1958) 1–34.

- [7] H.H. Korst, A theory for bases pressure in transonic and supersonic flow, *Trans. ASME J. Appl. Mech.* 23 (4) (1956) 593–600.
- [8] K. Karashima, Base Pressure on Two-dimensional Blunt-trailing-edge Wings at Supersonic Velocities 27, Aeronautical Research Institute, University of Tokyo, 1961, pp. 8–11.
- [9] W.L. Chow, On the base pressure resulting from the interaction if a supersonic external stream with a sonic or subsonic jet, *J. Aeronaut. Sci.* 26 (3) (1959) 176–180.
- [10] J.S. Anderson, T.J. Williams, Base pressure and noise produced by the abrupt expansion of air in a cylindrical duct, *J. Mech. Eng. Sci.* 10 (3) (1968) 262–268.
- [11] B.W. Martin, P.J. Baker, Experiments on a supersonic parallel diffuser, *J. Mech. Eng. Sci.* 5 (5) (1963) 98–113.
- [12] W.M. Jungowski, On the flow in a sudden enlargement of a duct, *Fluid Dyn. Trans.* 4 (1969) 231–241.
- [13] W.M. Jungowski, On the pressure oscillation in sudden enlargement of a duct section, *Fluid Dyn. Trans.* No. 1 (1967) 735–741.
- [14] P.K. Chang, Separation of Flow, Pergamon Press, Oxford, 1970 (In 3 volumes).
- [15] A.I. Shvets, I.T. Shvets, Gas Dynamics of the Near Wake, *Naukova Dumka*, Kiev, 1976, p. 380 (in Russian).
- [16] G.Yu Stepanov, L.V. Gogish, Quasi-One Dimensional Gas Dynamics of Nozzles of Jet Engines, *Mashinostroenie*, Moscow, 1973, p. 167 (in Russian).
- [17] A.M. Sizov, Gas Dynamics and Heat Transfer of Gas Jets in Metallurgic Processes, *Metallurgia*, Moscow, 1987, p. 256 (in Russian).
- [18] A.V. Yavovskiy, V.L. Yavovskiy, A.M. Sizov, Pulse Blowing Application to Steel Production, *Metallurgia*, Moscow, 1985, p. 176 (in Russian).
- [19] A.A. Shishkov, Gas Dynamics of Powder Rocket Engines, *Mashinostroenie*, Moscow, 1968, p. 148 (in Russian).
- [20] A.A. Shishkov, B.M. Silin, High-Altitude Tests of Jet Engines, *Mashinostroenie*, Moscow, 1985, p. 208 (in Russian).
- [21] W.M. Jungowski, Theoria abliczenie i badanie strumienicy gazawcy o zmiennym wydatki, *Arch. Budowy Masz. (Arch. Mech. Eng.)* 23 (3) (1976) 345–358 (in Polish).
- [22] W.M. Jungowski, K.J. Witzczak, Properties of an annular jet generating discrete frequency noise, *Arch. Mech.* 28 (5–6) (1976) 847–854.
- [23] J.S. Anderson, W.M. Jungowski, W.J. Hiller, G.E.A. Meier, Flow oscillation in a duct with a rectangular cross-section, *J. Fluid Mech.* 79 (4) (1977) 769–784.
- [24] W.M. Jungowski, Some self-induced supersonic flow oscillations, *Prog. Aerosp. Sci.* 18 (C) (1978) 151–175.
- [25] V.G. Dulov, G.A. Lukyanov, Gas Dynamics of Outflow Processes, *Nauka*, Novosibirsk, 1984, p. 232 (in Russian).
- [26] V.N. Glaznev, V.I. Zapryagaev, V.N. Uskov, N.M. Terekhova, V.K. Erofeev, V.V. Grigoryev, A.O. Kozhemyakin, V.A. Kotenok, A.V. Omelchenko, Jet and Unsteady Flows in Gas Dynamics, Siberian Branch of the RAS, Novosibirsk, 2000, p. 200 (in Russian).
- [27] P.V. Bulat, O.N. Zasukhin, V.N. Uskov, Mechanisms of unsteady processes in channel with abrupt expansion, in: *Proceedings of the 15th All-Union Seminar on Gas Jets*, Leningrad, 21. (in Russian), 1990.
- [28] G.V. Naberezhnova, Yu.N. Nesterov, Unstable interaction of expanding supersonic jet with an obstacle, *Proc. TsAGI* (1765) (1976) (in Russian).
- [29] V.A. Ostapenko, A.V. Solotchin, Power influence of supersonic underexpanded jet on a plane obstacle, *Proc. Sib. Branch Ras. Ser. Eng. Sci.* 13 (3) (1974) 26–32 (in Russian).
- [30] G.F. Gorshkov, V.N. Uskov, V.S. Favorskii, Nonstationary flow of an under-expanded jet around an unbounded obstacle, *J. Appl. Mech. Tech. Phys.* 34 (4) (1993) 503–508.
- [31] G.F. Gorshkov, V.N. Uskov, A.P. Ushakov, Oscillatory interaction between an underexpanded jet and an obstacle in the presence of supersonic sheathed flow, *J. Appl. Mech. Tech. Phys.* 32 (4) (1991) 512–518.
- [32] B.Sh Albazarov, Numerical Simulation of Supersonic Jet Interaction With an Obstacle (PhD Thesis), Leningrad State University, 1991, p. 190.
- [33] B.G. Semiletenko, B.N. Sobkolov, V.N. Uskov, Features of unstable interaction between a supersonic jet and infinite baffle, *Fluid Mech. Sov. Res.* 3 (1) (1974) 90–95.
- [34] V.N. Glaznev, Inverse feedback mechanism in self-oscillations in flow of an underexpanded supersonic jet against a planar obstacle, *J. Appl. Mech. Tech. Phys.* 32 (4) (1991) 519–522.
- [35] A Powell, The sound-producing oscillations of Round underexpanded jets impinging on normal plates, *J. Acoust. Soc. Am.* 83 (2) (1988) 515–533.
- [36] M.P. Bulat, P.V. Bulat, Comparison of turbulence models in the calculation of supersonic separated flows, *World Appl. Sci. J.* 27 (10) (2013) 1263–1266.
- [37] A.V. Omel'chenko, V.N. Uskov, M.V. Chernyshev, An Approximate analytical model of flow in the first barrel of an overexpanded jet, *Tech. Phys. Lett.* 29 (3) (2003) 243–245.
- [38] M.V. Silnikov, M.V. Chernyshov, V.N. Uskov, Two-dimensional over-expanded jet flow parameters in supersonic nozzle lip vicinity, *Acta Astronaut.* 97 (2014) 38–41.
- [39] A.V. Savin, E.I. Sokolov, N.B. Fedosenko, Circulation zones in a supersonic underexpanded jet flowing out of a nozzle with a cylindrical central finite-length body, *Fluid Dyn.* 50 (1) (2015) 33–39.
- [40] N.N. Smirnov, V.B. Betelin, V.F. Nikitin, L.I. Stamov, D.I. Altoukhov, Accumulation of errors in numerical simulations of chemically reacting gas dynamics, *Acta Astronaut.* 117 (2015) 338–355.
- [41] N.N. Smirnov, V.B. Betelin, R.M. Shagaliev, V.F. Nikitin, I.M. Belyakov, Yu.N. Deryuguin, S.V. Aksenov, D.A. Korchazhkin, Hydrogen fuel rocket engines simulation using logos code, *Int. J. Hydrog. Energy* 39 (20) (2014) 10748–10756.